$^{12}C+^{12}C$ elastic scattering excitation functions and phase shift analysis

R. J. Ledoux, M. J. Bechara,* C. E. Ordonez,
H. A. Al-Juwair, and E. R. Cosman
Laboratory for Nuclear Science, Massachusetts Institute of Technology, Cambridge, Massachusetts 02139
(Received 7 September 1982)

The $^{12}C+^{12}C$ elastic scattering has been measured for $E_{c.m.}=14.6$–31.3 MeV, $\theta_{c.m.}=30°$–$110°$. The elastic data have been analyzed via a phase shift analysis, enabling the extraction of model independent sets of phase shift parameters. The extracted J^{π} values for the intermediate structure resonances at $E_{c.m.}=18.4$, 19.3, and 20.3 MeV are 12^+, 12^+, and 12^+ or 14^+, respectively. The questions of ambiguities in the phase shift analysis and the comparison with J^{π} values deduced from other experiments are discussed. Evidence is presented for the existence of gross structure resonances. The elastic scattering has also been analyzed using the sum-of-differences method to directly extract the total reaction cross section. The results of these analyses are compared to existing models of the origin of intermediate structure resonances.

[NUCLEAR REACTIONS Measured the $^{12}C+^{12}C$ elastic scattering, $E_{c.m.}=14.6$–31.3 MeV, $\theta_{c.m.}=30°$–$110°$. Phase shift analysis, sum-of-differences analysis.]

I. INTRODUCTION

The study of the $^{12}C+^{12}C$ system has revealed the existence of resonant phenomena for energies from below to well above ($E_{c.m.}=48$ MeV) the Coulomb barrier. The spins and the elastic partial widths are known for many of these resonances in the Coulomb barrier region.[1,2] The elastic partial widths are significantly larger than those predicted[1–3] by the compound nucleus model, which prompted the first explanation[3,4] of these resonances as nuclear "molecular" resonances. More refined molecular models[5–8] and alternate models such as the α particle model,[9] although explaining certain qualitative aspects of the intermediate structure spectrum, have not provided a satisfactory explanation for the origin of these resonances.

The $^{12}C+^{12}C$ reaction has also been studied for energies well above the Coulomb barrier. The elastic scattering[10,11] and many reaction channels[12–16] (as well as the total reaction[17] and total fusion cross sections[17,18]) exhibit intermediate width structure. However, the large compound nucleus level density and the large number of open reaction channels make it difficult to discriminate between intermediate structure and compound-nucleus fluctuations. A statistical analysis[19] of the $^{12}C+^{12}C$ elastic scattering for $E_{c.m.}=13.5$–37.5 MeV indicated that the structures with widths between 200–800 keV were consistent with statistical model predictions. Therefore, if intermediate width structures are to be interpreted as intermediate structure resonances, cross correlations among channels must be found, preferably among angle integrated yields. (Feshbach[20] has pointed out that resonances need not be seen in every channel.) It is also important to ascertain if a unique spin can be associated with an intermediate width structure.

Cosman *et al.*[16] have recently compiled the existing data on the $^{12}C+^{12}C$ system for $E_{c.m.}=10$–35 MeV. They demonstrated that the intermediate width structure (300–800 keV) is correlated between the elastic and other reaction channels, particularly the inelastic[14] and the $\alpha+^{20}Ne$ channels.[13,17] The strong correlation of intermediate width structure makes plausible the interpretation of many of these structures as intermediate structure resonances.

Various models for the origin of intermediate structure have been proposed, such as fragmented shape resonances,[20] resonant inelastic coupling,[5–8] and shape isomeric states in ^{24}Mg.[12,21] In order to decide among these models, it is necessary to know the spins and partial widths of the intermediate structure. In particular, if the structures could be associated with a unique J^{π}, the resonance interpretation for these structures would be further verified. A reasonable choice of channel for the extraction of resonant spins is the elastic channel, not only because of its spin-zero, identical particle nature, but also by virtue of the dramatic correlated intermedi-

ate structure (IMS) observed in this channel. Measurements of the elastic channel also enable elastic partial widths to be extracted directly, assuming that spins are obtained unambiguously.

The results of the measurements and analysis of the $^{12}C+^{12}C$ elastic scattering for $E_{c.m.}=14.6$–31.3 MeV and $\theta_{c.m.}=30°$–$110°$ are presented in this paper. The elastic angular distributions were measured in 100 keV steps in the energy region $E_{c.m.}=17.8$–21.1 MeV. This region was studied in such detail because the elastic scattering had never been studied over much of this region and also because there exist three prominent intermediate width anomalies in this region. The remaining energy regions were studied in varying step sizes. All of the elastic angular distributions were analyzed with a phase shift analysis, in hopes of obtaining a model independent set of resonant and background phase shift parameters. The elastic data were also analyzed using the sum-of-differences method[22,23] to obtain a direct estimate of the resonant total reaction cross section. Before proceeding to a discussion of the details of the method and results of the phase shift analysis (Sec. III A), a summary of the experimental procedure used in making the elastic scattering measurements is described in the next section.

II. EXPERIMENTAL PROCEDURE

The $^{12}C+^{12}C$ elastic scattering measurements were performed in three sets of runs at the Brookhaven National Laboratory Tandem Van de Graaff Facility. All targets were self-supporting natural carbon foils, 10 $\mu g/cm^2$ areal thickness. The targets also had a small deposit of ^{197}Au (less than 1 $\mu g/cm^2$). The energy loss in the targets was always less than 30 keV (c.m.).

Elastic and reaction products were detected in bare silicon surface barrier detectors, which were placed on two plates located on opposite sides of the scattering chamber. Four detectors, separated by 5°, were positioned on each plate. The detectors had an angular acceptance of 0.5° (laboratory). The absolute angles were known to better than 0.5° (laboratory).

The energy signals from each plate were summed and input to a single analog-to-digital converter. Simultaneously, a logic signal was generated for each detector and input to a pattern generating device. Therefore, each event was associated with an energy signal and a number representative of the detector which detected the particle. Only non-pile-up events were recorded on-line. The relative percentage of pile-up events to single events was monitored and the beam intensity adjusted to keep this percentage less than 1%.

Relative cross-section normalization was achieved from the ratio of the measured $^{12}C+^{12}C$ and $^{12}C+^{197}Au$ elastic yields and the calculated $^{12}C+^{197}Au$ Rutherford cross sections. Absolute normalization was obtained by measuring the elastic scattering of ^{12}C at $E_{lab}=12.0$ MeV, $15°<\theta_{lab}<20°$, at the beginning and end of each experiment. The deviations from $^{12}C+^{12}C$ Mott scattering are known[23] to be less than 10% at $E_{lab}=12.0$ MeV. In order to minimize the effects of carbon buildup on the target, a cryogenic arm surrounded the target and helped provide a high vacuum. Repeat runs were performed to monitor the carbon buildup. The uncertainty in the absolute cross sections resulting from the uncertainty in target thickness and the $^{12}C+^{12}C$ Mott scattering is less than 15%.

The $^{12}C+^{12}C$ and $^{12}C+^{197}Au$ elastic peaks were well separated from other reaction products at most angles and energies. At the most forward angles, $\theta_{lab}<20°$, and at the most backward angles, $\theta_{lab}>45°$, there was a background due to light particle reaction products. Error bars have been calculated for all the data, taking into account the statistical error and any error due to overlap with reaction products or beam tail. The average relative uncertainty in cross sections was approximately 5%.

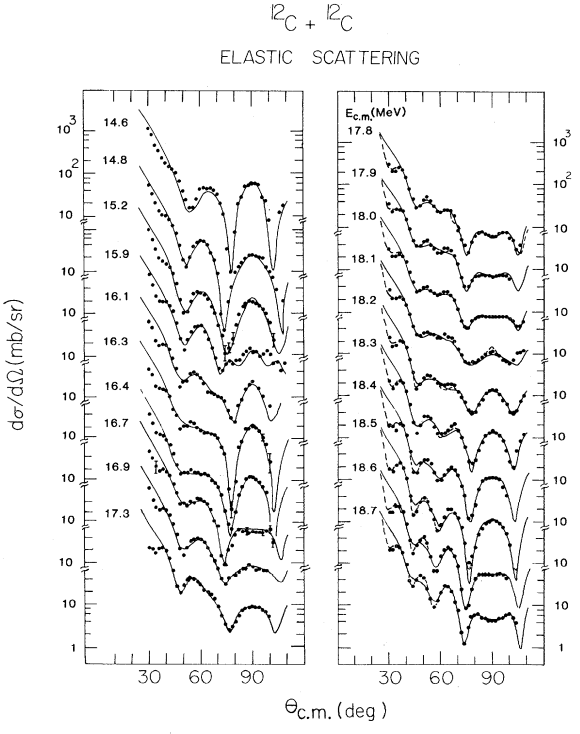

FIG. 1. $^{12}C+^{12}C$ elastic scattering data with zero phase (solid curve) and large phase (dashed curve) phase shift analysis fits.

III. RESULTS AND ANALYSIS

A. Phase shift analysis

The extracted $^{12}C+^{12}C$ elastic angular distributions are displayed in Figs. 1–3. The curves through the data points are fits obtained from a phase shift analysis of the data. It is obvious that the elastic angular distributions can significantly change their character with an energy variation of only 100 keV (c.m.) (e.g., the energy regions centered at $E_{c.m.}=18.4$, 19.3, and 20.3 MeV). The central question is whether these variations are indicative of resonant or nonresonant processes. An elastic phase shift analysis was performed in an attempt to answer this question. The details of the procedure and the results of this phase shift analysis are discussed in this section.

The elastic differential cross section for identical spin zero particles can be expressed as[2]

$$\frac{d\sigma}{d\Omega}=\left[\frac{Z^2e^2}{4E_{c.m.}}\right]^2\left|\frac{\exp\{-i\gamma\ln[\sin^2(\theta/2)]\}}{\sin^2(\theta/2)}+\frac{\exp\{-i\gamma\ln[\cos^2(\theta/2)]\}}{\cos^2(\theta/2)}\right.$$
$$\left.+\frac{2}{i\gamma}\sum_{l\ \text{even}}(2l+1)\exp[2i(\sigma_l-\sigma_0)][1-S_l(E)]P_l(\cos\theta)\right|^2, \quad (1)$$

where

$$\gamma=\alpha Z^2(\mu c^2/2E_{c.m.})^{1/2},$$

α is the fine structure constant, μ is the reduced mass, $S_l(E)$ are the elastic nuclear matrix elements, and σ_l are the Coulomb phase shifts for partial wave l. The S-matrix elements are parametrized by

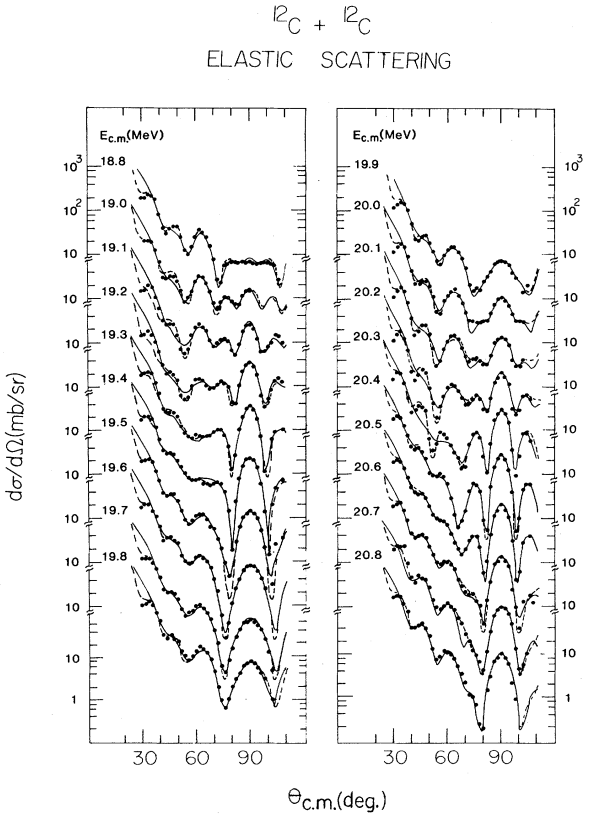

FIG. 2. Same as Fig. 1 except $E_{c.m.}=18.8$–20.8 MeV.

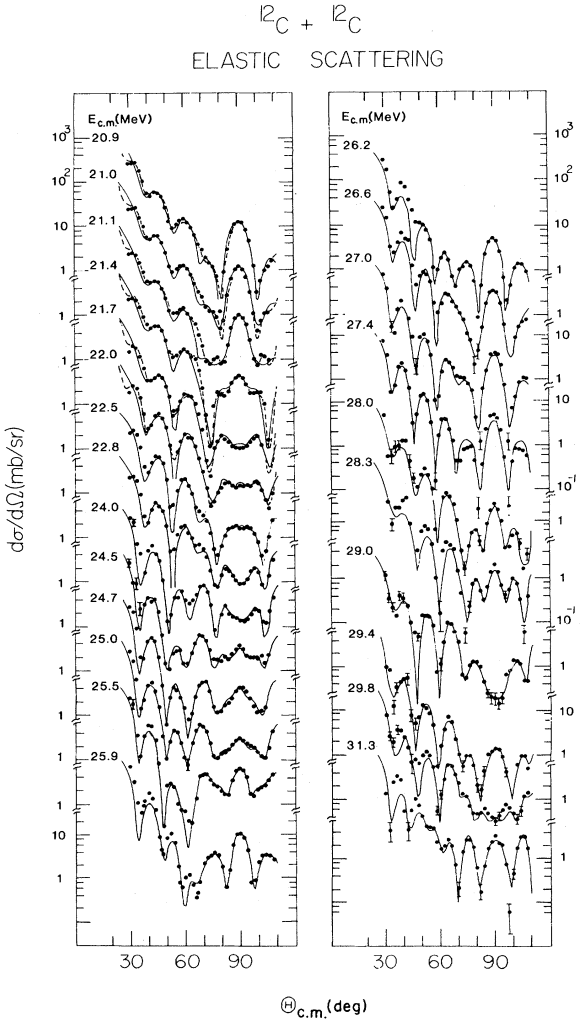

FIG. 3. Same as Fig. 1 except $E_{c.m.}=20.9$–31.3 MeV.

$$S_l(E)=\eta_l(E)e^{2i\delta_l(E)}, \tag{2}$$

where

$$\eta_l(E)=|S_l(E)| .$$

Here, η_l is referred to as the reflection coefficient for the lth partial wave, and δ_l as simply the phase. In terms of these parameters, the total reaction cross section is given by

$$\sigma_R=\frac{2\pi}{k^2}\sum_{l\ \text{even}}(2l+1)(1-\eta_l^2) . \tag{3}$$

The values of the nuclear S-matrix elements were obtained by varying η_l and δ_l such that a good fit was obtained simultaneously for both the elastic angular distributions and the total reaction cross section. One criterion used to determine the "goodness" of a fit is the value of the reduced χ-square (χ_ν^2). The χ_ν^2 has contributions from the elastic and total reaction cross sections and is given by

$$\chi_\nu^2=\frac{1}{N-n-1}\left[\sum_{i=1}^{N}\left[\frac{\sigma^{\text{fit}}(\theta_i)-\sigma^{\text{exp}}(\theta_i)}{\Delta\sigma(\theta_i)}\right]^2\right] + \left[\frac{\sigma_R^{\text{fit}}-\sigma_R^{\text{exp}}}{\Delta\sigma_R}\right]^2 , \tag{4}$$

where N is the number of experimental points and n is the number of free parameters (i.e., twice the number of partial waves allowed to vary) used in the phase shift analysis. The uncertainty in the total reaction cross section was chosen as a constant 25 mb. This value is a factor of 3 or 4 less than the true experimental uncertainty.[17] The use of an artificially small error in the total reaction cross section made the χ_ν^2 more sensitive to the total reaction cross section term. This helped ensure that all solutions (i.e., sets of phase shift parameters) found from the phase shift analysis also correctly reproduced the total reaction cross sections.

The search on the phase shift parameters was accomplished via a gradient search computer code which attempted to minimize the χ_ν^2. In the energy region from 14.6 to 22.8 MeV (c.m.) the $l=4$–18 partial waves were varied. The $l=6$–20 partial waves were varied for energies between 24.0 and 31.4 MeV (c.m.). Low partial waves which were not varied had fixed values of their scattering matrix elements: $\eta_l=0$, $\delta_l=0$ (i.e., totally absorbed). The grazing partial waves for $E_{\text{c.m.}}=20$ and 25 MeV are approximately 12 and 14, respectively. Therefore, the partial waves included in the calculations should account for all of the nuclear contributions to the scattering.

The approach taken to obtain phase shift parameters was basically a bootstrap method. The first region investigated was from $E_{\text{c.m.}}=18$ to 21 MeV. The phase shift parameters for contributing partial waves in the gradient search were initially varied with identical differential step sizes. Once a few angular distributions were fit, the fits were redone, this time attempting to constrain the phase shifts to their average values. This smoothing process occasionally resulted in slightly inferior fits to the angular distributions (i.e., larger values of the χ_ν^2). The exact compromise between the smoothness (with energy) of the phase shift parameters and the value of the χ_ν^2 was, of course, subjective (and consequently not unique). More energies were fit and the smoothing process was repeated. In this way the fits for all the angular distributions were slowly obtained. All partial waves were varied equally unless it was found that superior fits could be obtained by a more rapid variation of one partial wave.

One of the most important factors in each fit is the choice of the initial values of the phase shift parameters. The initial values of the reflection coefficients were chosen roughly according to sharp cutoff model predictions. Two strategies were used in selecting the initial values of the phases. The first strategy simply started all phases at 0° and allowed them to vary slowly (except for any resonant partial wave). The second strategy started the phases of low partial waves at large values (similar to optical model predictions[24,10]) and allowed them to vary more rapidly. (The differential step sizes for the reflection coefficients and nuclear phases could be varied independently in the gradient search.) Solutions based on these initial conditions have been explored in detail.

The phase shift parameters obtained from the phase shift analysis with the 0° phase initial condition are displayed in Fig. 4. The solid curves through the data in Figs. 1–3 were calculated using the phase shift parameters in Fig. 4. Before discussing this solution a few comments are in order. The reasons for attempting this "zero phase" solution were to reduce the number of free parameters in the fits and also to start the phases out at model independent initial conditions. [The number of free parameters, n, used in Eq. (4) was always taken as twice the number of partial waves allowed to vary, no matter how small the variation of the phases.] It is difficult to quantify the reduction in the effective number of free parameters which results from the enforced slow variation of the phases relative to the reflection coefficients. However, it was found that the angular distributions could be fairly well fit even with no variation of the phases, except on resonance. These observations indicate that there are enough free parameters in the reflection coefficients alone to fit the off-resonance data. Thus, there exist ambi-

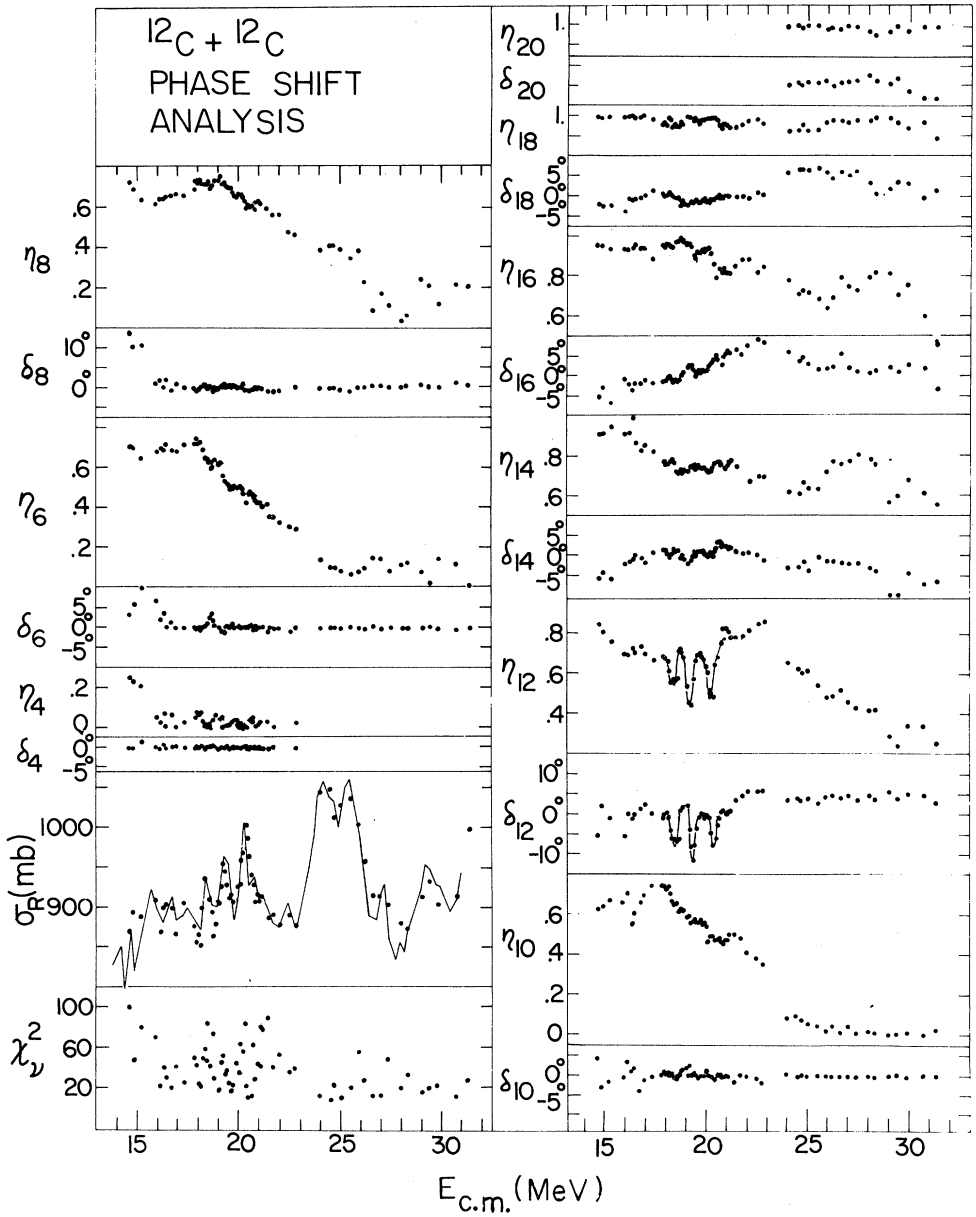

FIG. 4. Results of $^{12}C+^{12}C$ elastic phase shift analysis using zero phase initial condition (see text). The experimental total reaction cross section (solid curve) is taken from Ref. 17.

guities in the extracted background phase shift parameters.

A systematic problem with this particular solution was the inability to simultaneously fit the elastic angular distributions for $30° < \theta_{c.m.} < 40°$ and $40° < \theta_{c.m.} < 90°$. Therefore only the $40° < \theta_{c.m.} < 90°$ data were included in the gradient search and in the evaluation of the χ_ν^2. As will be shown below, this problem most likely results from the use of background phases δ_l which are near zero. Another contribution to this discrepancy may result from the use of a point charge form factor and Coulomb phase shifts in Eq. (1).

With the above considerations in mind, we may now turn back to the phase shifts displayed in Fig. 4. The phase shift parameters are seen to generally vary smoothly as a function of energy, except for certain anomalies in some partial waves, the most striking of which is the dramatic variations with energy of the phase shift parameters of the $l = 12$ par-

tial wave. Both the phase and reflection coefficient for this partial wave go through correlated energy variations between $E_{\text{c.m.}}=17.8$–21.0 MeV. This energy region could not be fit well (using the present background) unless both η_{12} and δ_{12} were allowed to vary rapidly with energy relative to the other partial waves. The structures in the $l=12$ partial wave are centered at 18.4, 19.3, and 20.3 MeV, which correspond to energies where intermediate structures have been observed[12–16] in various reaction channels as well as in the total reaction cross section[17] (shown in Fig. 4 as a solid curve). There are also structures at $E_{\text{c.m.}}\sim 16.3$ MeV for the $l=10$ partial wave, at $E_{\text{c.m.}}\sim 29.4$ MeV for $l=14$, and at $E_{\text{c.m.}}\sim 25.5$ MeV for $l=16$. Thus it is possible to conjecture that the energies at which the above anomalies occur may correspond to resonant energies. For the anomalies in the $l=12$ partial wave this is a reasonable conjecture since intermediate width anomalies are known to be present at the three energies cited above. The structures at $E_{\text{c.m.}}=16.3$, 25.5, and 29.4 MeV are also correlated with structures observed in other channels. Unfortunately, the elastic data were not taken in fine enough steps to enable an extraction of spin values of these structures from the elastic phase shift analysis.

The reflection coefficient and the phase for the $l=12$ partial wave vary rapidly with energy in the energy region $E_{\text{c.m.}}=17.8$–21.0 MeV. However, it is important to determine if they do so in a resonant way. To illustrate some of the properties of a resonant S matrix, we will use the Breit-Wigner single level resonance formula as an example. The Breit-Wigner S matrix is given by

$$S_l(E)=\langle S_l(E)\rangle\left[1-e^{i\phi}\frac{i\Gamma_{\text{el}}}{(E-E_{\text{res}})+i\Gamma/2}\right], \tag{5}$$

where $\langle S_l\rangle$ is the background S matrix (assumed to vary slowly relative to the width of the resonant term). Γ_{el} and Γ are the elastic partial width and the total width, respectively, and ϕ is the mixing phase. In the complex plane (Argand diagram), the S matrix describes a closed circular loop (if the background amplitude does not vary over the resonance). The radius of the loop is dependent on Γ_{el} and the magnitude of the background S matrix. Relative to a point inside the loop, the phase δ_l of the S matrix varies by π [using the definition of the phase in Eq. (2)]. However, relative to the origin, the S matrix may vary by less than $\pi/2$. As a concrete example consider a Breit-Wigner resonance in the $^{12}C+^{12}C$ elastic scattering at $E_{\text{c.m.}}=19.3$ MeV, $\Gamma_{\text{el}}=100$ keV, $\Gamma=400$ keV, and $|\langle S\rangle|=0.75$. If the elastic scattering is measured in 100 keV steps, the maximum deviation in the phase of the S matrix observed would be 20°. Therefore, even resonances with large elastic widths will not necessarily be associated with large deviations in the phase of the resonant partial wave. This makes an unambiguous determination of the resonant spin difficult if the elastic width is not large or if there is appreciable background absorption.

The Argand diagram for the $l=12$ partial wave is displayed in Fig. 5 for $E_{\text{c.m.}}=17.8$–21.1 MeV. The diagram reveals the existence of three resonances with half widths of approximately 400 keV. The Argand diagrams for the three resonances are relatively simple and form essentially closed loops. Therefore it is reasonable to estimate the elastic partial width using the Breit-Wigner single resonance formula (5), on resonance and with zero mixing phase[2]:

$$\Gamma_{\text{el}}/\Gamma=\frac{1}{2}\left[1\pm\frac{\eta_l}{\langle\eta_l\rangle}\right];\begin{cases}+\text{ for }\dfrac{\Gamma_{\text{el}}}{\Gamma}>\dfrac{1}{2}\\ -\text{ for }\dfrac{\Gamma_{\text{el}}}{\Gamma}<\dfrac{1}{2}\end{cases}. \tag{6}$$

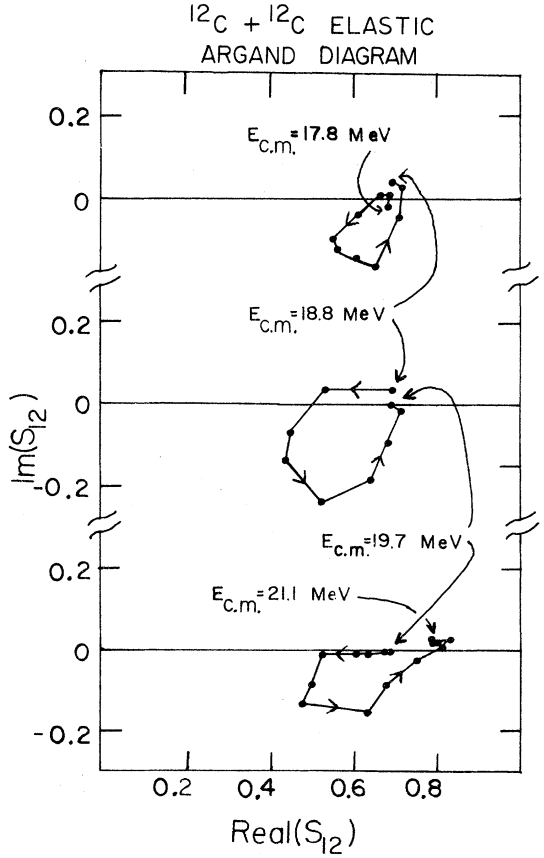

FIG. 5. Argand diagram for the $l=12$ partial wave for the zero phase solution (see text).

TABLE I. $^{12}C+^{12}C$ elastic scattering resonant properties. γ_{el}^2 is the elastic reduced width and γ_w^2 is the Wigner limit for the elastic channel. R_c is taken to be 5.7 fm for all calculations.

E_{res}	J^π	η_l^{res}	$\langle\eta_l\rangle$	Γ_{tot} (keV)	Γ_{el}/Γ_{tot}	γ_{el}^2 (keV)	γ_{el}^2/γ_w^2
			Zero phase solution				
18.4	12^+	0.55	0.74	400	12.8%	40	12.6%
19.3	12^+	0.45	0.74	400	19.6%	39	12.2%
20.3	12^+	0.50	0.74	400	16.2%	23	7.2%
			Large phase solution				
18.4	12^+	0.51	0.68	450	12.5%	45	14.0%
19.3	12^+	0.41	0.64	400	18.0%	36	11.4%
20.3	14^+	0.53	0.74	300	14.2%	100	31.6%

The extracted elastic partial widths, reduced widths, and the ratio of the reduced widths to the Wigner limits, obtained from the zero-phase solution, are given in the upper portion of Table I. The reduced widths account for approximately 10% of the Wigner limit for the elastic channel. Therefore, these resonances have a large $^{12}C+^{12}C$ parentage, as do the Coulomb barrier resonances.

The above results demonstrate that the elastic angular distributions and the total reaction cross section in the energy region $E_{c.m.}=17.8$–21.1 MeV can be well fit by three $l=12$ resonances and a smoothly varying (in energy) background. The question which must now be addressed is, are there significant ambiguities in the phase shift parameters?

The possiblity that the apparent resonant behavior in the elastic and total reaction cross sections is the result of the variation with energy of more than one partial wave has also been investigated for $E_{c.m.}=17.8$–21.1 MeV. As a starting point for the search for a new solution, the phase shift parameters for all except the $l=12$ partial wave were started at the values obtained in the solution discussed above. The $l=12$ phase shift parameters were made to vary more slowly than those for other partial waves. It was found that only the initial condition, $\eta_{12}\sim 0.80$ and $\delta_{12}\sim 0.0$, yielded a new solution. No attempt was made in this solution to smooth the variation with energy of the phase shift parameters. The phases were allowed to vary as freely as the variation of the reflection coefficients.

The phase shift parameters and the fit to the total reaction cross section are displayed in Fig. 6. The resonances at 19.3 and 20.3 MeV can be fit by allowing the $l=12$ reflection coefficient to be almost totally reflected while the $l=8$ and 10 reflection coefficients go through rapid variations with energy. The dips in the $l=8$ and 10 reflection coefficients are not accompanied by correlated variations in their phases. There is also structure in the $l=14$ and 16 phase shift parameters. The resonance at $E_{c.m.}=18.4$ MeV could not be fit without allowing the absorption of the $l=12$ partial wave. However, by not constraining the phase shift parameters to be smoothly varying, it is possible to remove the associated variation of the $l=12$ phase. The smaller values of the χ_ν^2 for this solution also result from

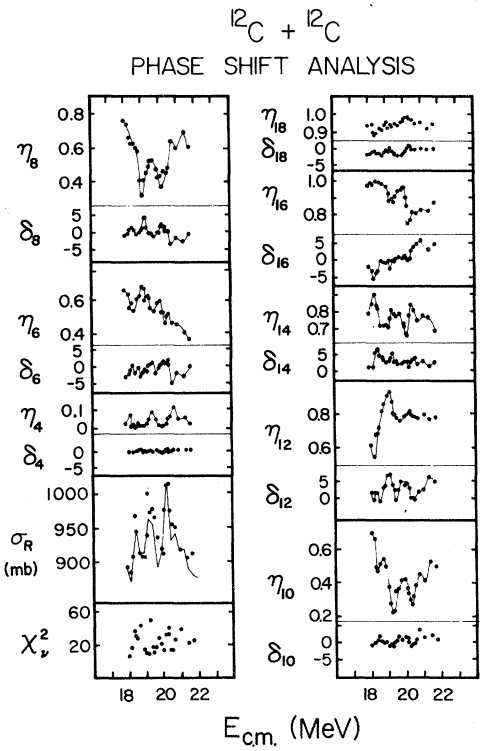

FIG. 6. Unconstrained phase shift analysis with $\eta_{12}=0.80$ and $\delta_{12}=0.0$ initial condition. The experimental total reaction cross section (solid curve) is from Ref. 17.

the fact that no attempt was made to smooth the phase shift parameters.

The finding of this second solution once again illustrates that there are ambiguities in the phase shift parameters. However, these two solutions both have something in common, that is, they require an unusual behavior for the phase shift parameters of the $l=12$ partial wave. The zero phase solution yielded three $l=12$ intermediate structure resonances. An alternate solution could be obtained only if the $l=12$ partial wave was reflected for $E_{\text{c.m.}}=19$–21 MeV and resonantly absorbed for $E_{\text{c.m.}}=17.8$–19.0 MeV. This second solution may represent a mathematically equivalent representation (at least in describing the elastic and total reaction cross section) of the first resonant solution, which is possible because of the large number of phase shift parameters used in the fits. Thus, acknowledging the existence of ambiguities in the extracted phase shift parameters, we believe that little can be learned from a completely unconstrained search. A much more fruitful approach is to look for resonant (i.e., resonant variation of one partial wave) solutions using different initial conditions for the phase shifts.

Optical model calculations[10] and the phase shift analysis of Emling *et al.*[24] suggest that the phases δ_l for the low partial waves (i.e., $l=0$–8 for $E_{\text{c.m.}}=14$–19 MeV) obtain large values. Starting with background phases similar to those obtained by Emling *et al.*,[24] we have obtained a new solution for the energy region $E_{\text{c.m.}}=17.8$–22.0 MeV. The phase shifts and fit to the total reaction cross section are displayed in Fig. 7. It is important to notice that the χ_ν^2 are usually a factor of 2 better for this fit, as

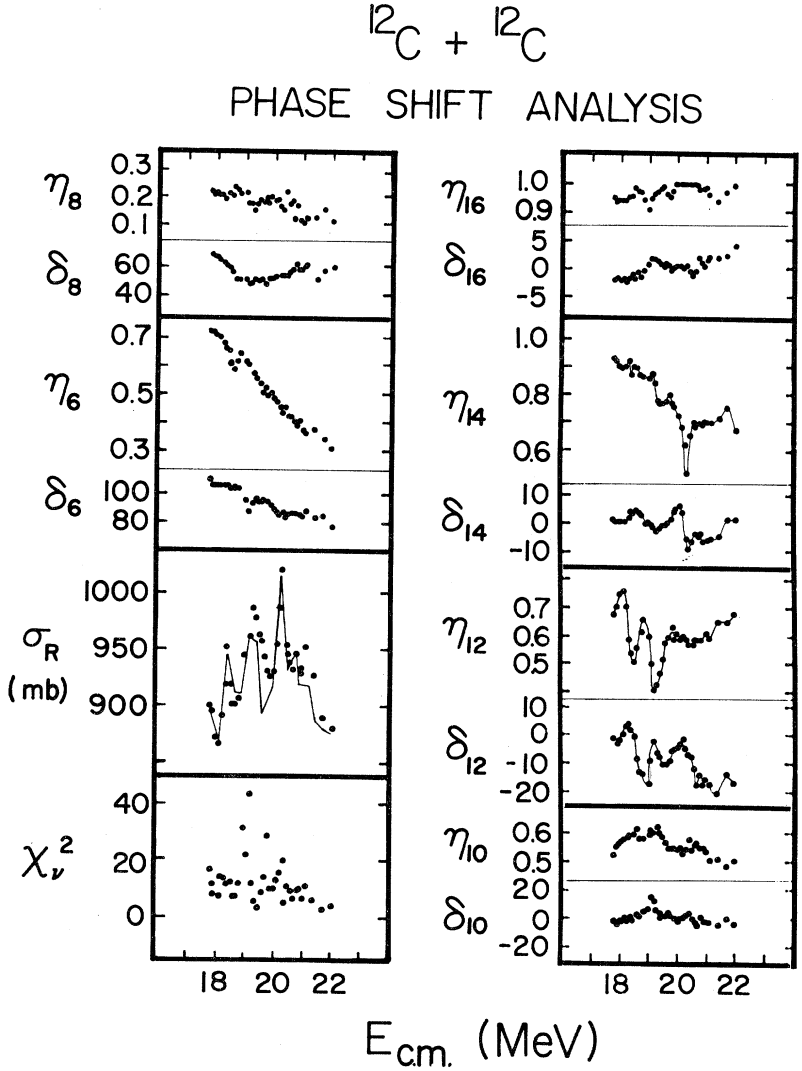

FIG. 7. $^{12}C+^{12}C$ elastic phase shift analysis with large phase initial condition (see text). The experimental total reaction cross section (solid curve) is from Ref. 17.

compared to those for the zero phase solution, discussed above. The fits to the elastic data for this solution are displayed in Figs. 1–3 as dashed curves. It is apparent that this "large phase" solution does a superior job at fitting the data, particularly the forward angle data. These improvements over the zero phase solution indicate that the phase shifts obtained in this solution more closely represent the true phase shifts.

An examination of Fig. 7 reveals the existence of $J^\pi=12^+$ resonances at $E_{c.m.}=18.4$ and 19.3 MeV and a $J^\pi=14^+$ resonance at $E_{c.m.}=20.3$ MeV. These are the same resonant energies as found in the zero phase solution for the three $J^\pi=12^+$ resonances (Fig. 4). Except for the values of the phases for the $l=6$ and 8 partial waves, the phase shift parameters for the two solutions are, on the average, very similar. Therefore, it is surprising that ambiguities exist for the spin assignment of the resonance at $E_{c.m.}=20.3$ MeV.

The Argand diagrams for the $l=12$ and 14 partial waves are displayed in Fig. 8. The $J^\pi=12^+$ resonance centered at 18.4 MeV does not form a closed loop and appears to possess a larger width than that extracted in the zero phase solution (Fig. 5). The $J^\pi=12^+$ resonance at $E_{c.m.}=19.3$ MeV does form a closed loop, but does so in a rather complicated manner (unlike a Breit-Wigner resonance which would form a circular loop). The complicated curves formed by the $E_{c.m.}=18.4$ and 19.3 MeV resonances may result from an overlap of these two

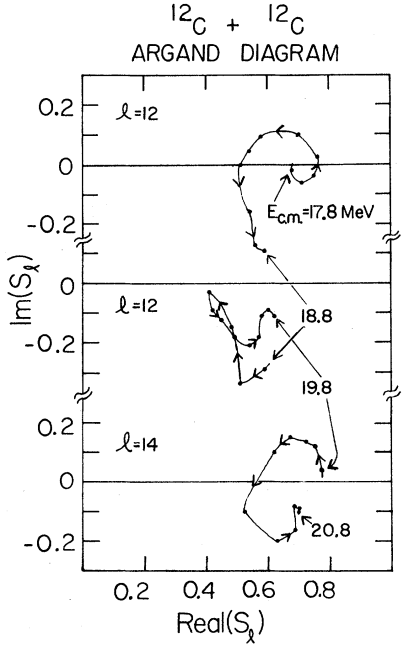

FIG. 8. Argand diagram for the $l=12$ ($E_{c.m.}=17.8$–19.8 MeV) and $l=14$ ($E_{c.m.}=19.8$–20.8 MeV) partial waves for the large phase solution.

resonances. This is plausible since the region which complicates the forming of closed loops is centered near $E_{c.m.}=18.8$ MeV, which is the overlap region of the two resonances. The Argand diagram for the $l=14$ partial wave over the $E_{c.m.}=20.3$ MeV resonance has an almost circular structure that does not completely close. This behavior can be attributed to a slow absorption of the background S matrix for this partial wave.

Although the Argand diagrams do not form simple circular loops, we have used the Breit-Wigner form of the S matrix to extract approximate elastic partial and reduced widths [Eq. (6)]. The extracted values of Γ_{el} and γ_{el}^2 are listed in the lower portion of Table I. The values of Γ_{el} are very similar for both the zero phase and large phase solutions. Even the 20.3 MeV resonance, for which different spin assignments have been obtained, has roughly the same elastic partial width in both solutions. The lack of dependence of the elastic width on the particular set of phase shift parameters (which we assume adequately fits both the elastic and total reaction cross section data) probably results from the constraint that the absorption of only one partial wave may account for resonances in the total reaction cross section. However, the decreased penetrability for a $J^\pi=14^+$ resonance, as compared to a $J^\pi=12^+$ resonance at $E_{c.m.}=20.3$, yields a significantly larger reduced width. Thus, it has been found that the use of large phases for the $l=6$ and 8 partial waves yield superior fits to the elastic data and a $J^\pi=14^+$ assignment for the $E_{c.m.}=20.3$ MeV resonance. In light of the improved fit obtained in the large phase solution, the $J^\pi=14^+$ assignment for the $E_{c.m.}=20.3$ MeV resonance is favored over the $J^\pi=12^+$ assignment obtained for this resonance in the zero phase solution. However, the problem of ambiguities in the phase shift parameters (and hence spin assignments) cannot be eliminated from the analysis of the available elastic and total reaction cross section data.

An independent source of information on the spin assignments for the three resonances in the energy region $E_{c.m.}=17.8$–21.1 MeV is found in the branching ratios observed in particle decay channels. The 19.3 MeV resonance has been found to be consistent with a $J^\pi=12^+$ assignment by a number of authors.[12,14,15] The 20.3 MeV resonance has been found[12] to have no decay to the 9.81 MeV ($17/2^+$) state in ^{23}Na and the 4.45 MeV (7^+) state in ^{22}Na. Considering the strong decays to these states, for the 19.3 MeV resonance two conclusions are possible. The simplest conclusion is that the resonance at 20.3 MeV has $J>12$. A second conclusion is that there are structural differences between the two resonances which dominate any statistical selection

rules. Therefore, the superior $J^\pi = 14^+$ fit in the phase shift analysis and the p and d decays suggest that a $J^\pi = 14^+$ assignment for the 20.3 MeV resonance is most simply consistent with the data. There are no indications that the 19.3 MeV resonance is anything but $J^\pi = 12^+$.

Studies of the $^{12}C(^{12}C,Be(g.s.))^{16}O$ (Refs. 15 and 25) and $^{12}C(^{12}C,\alpha_0)^{20}Ne$ (Ref. 25) reactions over the 18.4 MeV resonance yield conflicting spin values. The α decay is consistent with $J^\pi = 10^+$ while the ^{8}Be (g.s.) channel favors $J^\pi = 12^+$. The elastic phase shift analysis yields $J^\pi = 12^+$ for the 18.4 MeV resonance, which is consistent with the ^{8}Be (g.s.) decay. The $J^\pi = 10^+$ assignment obtained from the α channel could either reflect the existence of an almost degenerate $J^\pi = 10^+$ resonance or a small resonance decay width which could allow a small anomaly to be seen in a single angle excitation function but could have little effect on the dominant l value deduced from the angular distributions. At these energies the dominant l wave (grazing) for α decay to the ^{20}Ne ground state is $l = 10$ (Ref. 25) so that this would be likely to dominate all angular distributions. Thus, the $J^\pi = 12^+$ assignment obtained from the three phase shift analysis solutions is also consistent with the particle decay data. In the discussion section of this paper we will address the implications of the spin assignments discussed above.

Our attention so far has been focused on the possible ambiguities in the spin assignments. The main source of these ambiguities is the uncertainty in the background phase shifts. In particular, different initial conditions in the background phases lead to different spin assignments for the 20.3 MeV resonance. However, what is surprising is that the reflection coefficients for the three phase shift solutions are, on the average, remarkably similar. Also of interest is the fact that although the initial conditions for the reflection coefficients were similar to those of the sharp cutoff model (or those of commonly used optical models[10,24]), the final reflection coefficients always differed greatly from these initial conditions. (They also differ from recent folding model calculations.[26])

Figure 9 displays the reflection coefficients from the large phase solution for the $l = 14$ and 16 partial waves for $E_{c.m.} = 17.8$–22.0 MeV. The reflection coefficients for the $l = 6$–12 partial waves are merged with the reflection coefficients obtained by Emling *et al.*[24] in the region $E_{c.m.} = 16.0$–18.8 MeV. The reflection coefficients for all partial waves above $E_{c.m.} = 22.8$ MeV are from the zero phase solution. However, it is important to emphasize that there is essentially only one phase shift solution for $E_{c.m.} > 22.0$ MeV. The reason for this is that the $l = 6$ and 8 partial waves are almost completely absorbed above 22.0 MeV. Therefore, the values of these phases are unimportant. The average trend in the reflection coefficients for both the large and zero phase solutions are very similar. There are no indications in either solution that the phases for $l > 8$ obtain large values. Thus, until elastic data are taken in finer energy steps for $E_{c.m.} > 22.0$ MeV, only one phase shift solution can be extracted.

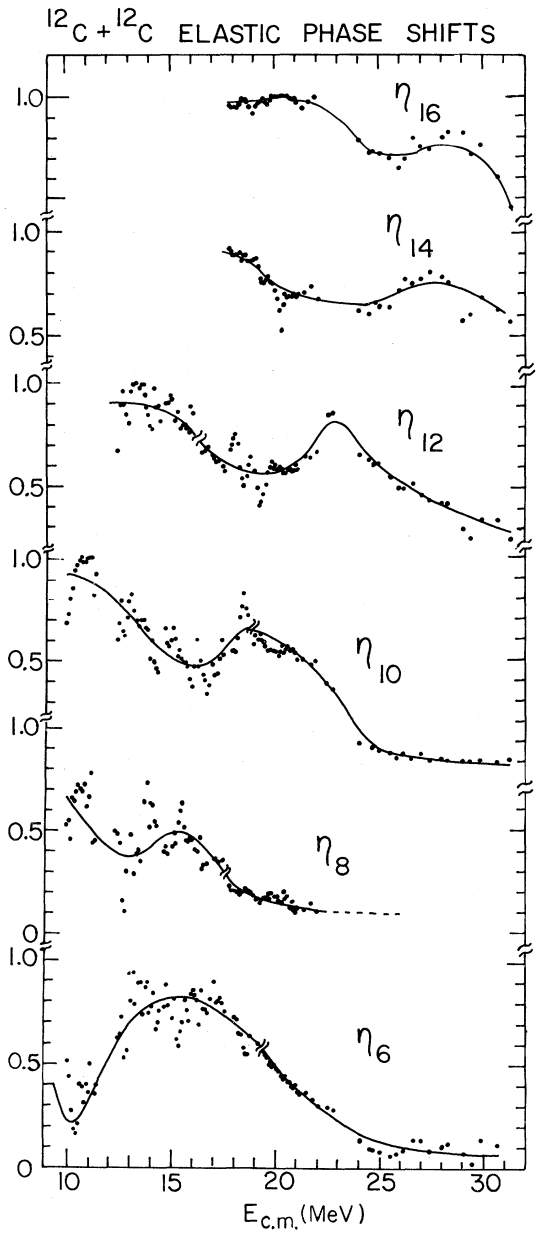

FIG. 9. Reflection coefficients from the present phase shift analysis and those of Emling *et al.* (Ref. 24). The curve is drawn to guide the eye.

The most important feature of Fig. 9 is the average energy dependence of the reflection coefficients.

Each partial wave shows evidence of enhanced absorption over a range of a few MeV. The gross structures in the $l=14$ and 16 partial waves are on the order of 4 MeV wide and appear to overlap. There is a general trend toward wider regions of enhanced absorption with increasing angular momentum and energy. As mentioned above, the average reflection coefficients are very similar for all solutions. Therefore, Fig. 9 presents model independent evidence that gross structure effects result from the action of one partial wave (for $l<14$) in a given energy region.

B. Sum-of-differences

There is a very simple and direct way of extracting the total reaction cross section from elastic scattering data. Wojciechowski *et al.*[22] have shown that the total reaction cross section for heavy-ion reactions may be obtained from the following approximate expression (which has been modified for identical particles[23]):

$$\sigma_R^{\mathrm{SOD}}=2\pi\int_{\theta_0}^{\pi/2}\left[\frac{d\sigma_M}{d\Omega}-\frac{d\sigma_{\mathrm{el}}}{d\Omega}\right]\sin\theta\,d\theta\ , \tag{7}$$

where $d\sigma_M/d\Omega$ and $d\sigma_{\mathrm{el}}/d\Omega$ are the Mott and experimental elastic cross sections, respectively. This method of obtaining the total reaction cross section is called the sum-of-differences (SOD) method. It is a reliable method of extracting the total reaction cross section as long as $\theta_0<\theta_{\mathrm{grazing}}$ and both the Sommerfeld parameter and the absorption are large.[22,23]

Treu *et al.*[23] have measured the $^{12}C+^{12}C$ elastic scattering for $E_{\mathrm{c.m.}}=5.5$–12.0 MeV and have extracted σ_R^{SOD}. The absolute value of σ_R^{SOD} exceeds by as much as a factor of 2 the value σ_R obtained by γ-ray measurements.[1,27] The reason for this discrepancy is not clear. It may be that the absorption and/or the Sommerfeld parameter are not large enough in the region of the Coulomb barrier to satisfy the assumptions of Eq. (7). However, what is most important for our discussion is the fact that σ_R^{SOD} exhibits pronounced resonant structure which is well correlated with resonances observed in the elastic, $\alpha+^{20}Ne$, and $^{8}Be+^{16}O$ channels.

Figure 10 presents the results of a SOD analysis of the $^{12}C+^{12}C$ elastic data and also the total reaction cross section measurements of Kolata *et al.*[17,27] and the 90° c.m. elastic excitation function[10] for comparison. The full angular range of the elastic data, $\theta_{\mathrm{c.m.}}=30°$–90°, was used. The elastic data of Treu *et al.* were used for $E_{\mathrm{c.m.}}<15$ MeV. The center of mass energy corresponding to a classical

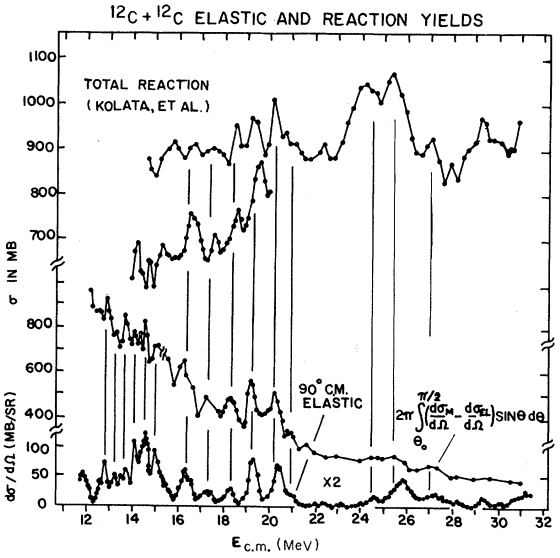

FIG. 10. The total reaction cross section as deduced from the $^{12}C+^{12}C$ elastic scattering using the sum-of-differences (SOD) method (Refs. 22 and 23). The experimental total reaction cross section (Refs. 17 and 27) and the 90° c.m. elastic excitation function (Refs. 10 and 11) have been included for comparison.

grazing angle of 30° (c.m.) is 22 MeV. Therefore, for $E_{\mathrm{c.m.}}<22.0$ MeV, the most important contributions to σ_R as derived from Eq. (7) are already included.

The total reaction cross section as predicted by the SOD method exhibits a decreasing cross section with increasing energy. The absolute value of σ_R^{SOD} is within error bars of σ_R^{exp} for $E_{\mathrm{c.m.}}\sim 15$ MeV. At higher energies σ_R^{SOD} drops below σ_R^{exp}. This may result from the loss of contributions to Eq. (7) from angles forward of $\theta_{\mathrm{c.m.}}=30°$. To test this, we have calculated σ_R^{SOD} using data from $40°<\theta_{\mathrm{c.m.}}<90°$, and have found approximately a 100–200 mb decrease in σ_R^{SOD}. Thus the decrease in the average σ_R^{SOD} suggests that there are significant deviations from Mott scattering forward of the classical grazing angle. This indicates that a more complete phase shift analysis than the one presented above would have to include elastic data for $\theta_{\mathrm{c.m.}}<30°$ for $E_{\mathrm{c.m.}}>16$ MeV.

The dramatic IMS resonances observed in the total reaction cross section are equally apparent in the total reaction cross section as extracted using the SOD method. There is a one-to-one correspondence between IMS observed in σ_R^{exp},[17,27] σ_R^{SOD}, and the 90° c.m. elastic excitation function.[10,11] This confirms that the dramatic variations with energy in the elastic scattering angular distributions are related to the presence of IMS resonances and that the resonances

which are prominent in the elastic scattering are the same as the resonances most prominent in the total reaction cross section.

IV. DISCUSSION

The $^{12}C+^{12}C$ elastic scattering is characterized by angular distributions which vary rapidly with energy, particularly in the energy region $E_{c.m.}=18-21$ MeV. Two sets of nuclear phase shifts have been found which reproduce the variation with energy of the elastic angular distributions by the resonant variation of one partial wave and the smooth variation of all others. The zero phase solution contains three $J^{\pi}=12^{+}$ resonances at $E_{c.m.}=18.4$, 19.3, and 20.3 MeV. The large phase solution also possesses $J^{\pi}=12^{+}$ resonances at $E_{c.m.}=18.4$ and 19.3 MeV, but yields a $J^{\pi}=14^{+}$ assignment for the 20.3 MeV resonance. Although the superior quality of the large phase solution and particle reaction data favor the $J^{\pi}=14^{+}$ assignment for the $E_{c.m.}=20.3$ MeV resonance, enough ambiguities exist that a consideration of the implications of either spin assignment is necessary.

Three $J^{\pi}=12^{+}$ resonances with large elastic partial widths (see the upper portion of Table I) clustered within 2 MeV is consistent with the existence of a fragmented elastic shape resonance.[15,20] The fragmentation of elastic shape resonances by inelastic coupling has been considered by many authors,[5-8] most recently in the band crossing model (BCM).[7] It is possible by the use of certain surface transparent potentials to obtain fragmentation of an elastic $J^{\pi}=12^{+}$ shape resonance in the $^{12}C+^{12}C$ system, although the number and widths of the predicted intermediate structures are not exactly reproduced. As such, the BCM allows a framework by which to understand the three $J^{\pi}=12^{+}$ intermediate width resonances obtained in the zero phase solution.

However, it is important to point out that the average phase shift parameters obtained in the present analysis differ substantially from those obtained from either the optical model potentials used in the BCM (Refs. 7 and 28) or earlier optical model potentials.[10] These potentials yield reflection coefficients which, for surface partial waves, vary rapidly (i.e., within a few MeV) from 1 (totally reflected) to 0 (totally absorbed). The average reflection coefficients displayed in Fig. 9 do not exhibit this behavior. Each partial wave is active over a large energy region, and many partial waves significantly contribute to the nuclear scattering amplitude at any given energy. Thus although the phase shift analysis yields gross structure resonances, the scattering amplitude is not dominated by a single partial wave.

There are aspects of particle decay channels, notably the proton and deuteron channels, which are not easily understood if both the $E_{c.m.}=19.3$ and 20.3 MeV resonances are $J^{\pi}=12^{+}$ resonances. The dramatic variations of the proton and deuteron decay over the 19.3 and 20.3 MeV resonances have already been discussed in Sec. III A. To date, the BCM has not made specific predictions about particle decay channels, although it is conceivable that channels other than the elastic and inelastic could be added to the calculations. The addition of $p+^{23}Na$ bands could potentially account for the selectivity for decay to certain high-spin excited states, but it seems unlikely that it could explain the strong variations in decay strengths over the 19.3 and 20.3 MeV resonances, assuming $J^{\pi}=12^{+}$ assignments for both resonances.

The existence of a $J^{\pi}=14^{+}$ resonance at $E_{c.m.}=20.3$ MeV has not as yet been incorporated into any model of the origin of intermediate structure in the $^{12}C+^{12}C$ system. The BCM cannot naturally explain the existence of a $J^{\pi}=12^{+}$ and 14^{+} resonance with large elastic reduced widths (see the lower portion of Table I) located within 1 MeV. However, the close proximity of a $J^{\pi}=12^{+}$ and 14^{+} resonance does not preclude the existence of elastic shape resonances. This is illustrated in Fig. 9, which includes the phase shift parameters from the large phase solution (which yields a $J^{\pi}=14^{+}$ assignment for the $E_{c.m.}=20.3$ MeV resonance), where the average energy variation of the reflection coefficients is consistent with the existence of elastic shape resonances. The existence of adjacent resonances of different J^{π} suggests that the origin of the intermediate structure may result from a mechanism different from that which leads to the elastic gross structure resonances. Degrees of freedom other than the elastic and inelastic channels may be important to any description of the reaction mechanism and resonant wave function.

Recent measurements[29] of the $^{12}C(^{12}C,\alpha)^{20}Ne^{*}$ reaction demonstrate that the ratio of α reduced widths to the Wigner limit for decay to certain excited ^{20}Ne states is comparable to similar ratios for the elastic and inelastic channels. Therefore, certain $\alpha+^{20}Ne^{*}$ configurations must be included in any description of the origin of intermediate structure in the $^{12}C+^{12}C$ system. Both the existence of a relatively complex spectrum of IMS resonances and the large and selective decay to special $\alpha+^{20}Ne^{*}$ configurations can qualitatively be included in a model which describes[29] the IMS resonances as states in a secondary minimum of the ^{24}Mg potential energy surface.[21] A complex spectrum of IMS resonances would result from excitations within this secondary minimum. For example a rotational-vibrational

spectrum with a $K^\pi=0^+$ band and $K^\pi=2^+$ γ-vibrational band could conceivably account for the close proximity of prominent $J^\pi=12^+$ and 14^+ resonances. The selective resonant α decay would result from the decay of these "shape-isomeric" states in ^{24}Mg to those in ^{20}Ne. Deformed shell model calculations[21] do, in fact, predict minima in the potential energy surface of ^{24}Mg and ^{20}Ne, which differ by a $(2p,2n)$ configuration, thus explaining the enhanced α decay to special ^{20}Ne states. Furthermore, the rotational band based on the predicted ^{24}Mg axially asymmetric secondary minimum[21,29] closely tracks the spectrum of known intermediate structure resonances (including the Coulomb barrier resonances), and Chandra and Mosel[30] have demonstrated that this axially asymmetric configuration has a large overlap with the $^{12}C+^{12}C$ entrance channel.

The above description of the origin of intermediate structure resonances in terms of shape-isomeric states in secondary minima of the ^{24}Mg potential energy surface is, with the present knowledge of spins and reduced widths, speculative. Its advantage over other models is that it is able in a natural way to explain a more complicated spectrum of IMS resonance as well as nonstatistical decays to special $\alpha+^{20}Ne^*$ configurations. However, before any one model may be favored over another, ambiguities in the spin assignment for the $E_{c.m.}=20.3$ MeV resonance must be removed. Also, spin assignments and reduced widths must be obtained for as many IMS resonances as possible, particularly in the energy region where $J^\pi=8^+-12^+$ resonances are already known.

The results presented in this paper demonstrate that, although not entirely free from ambiguities, a phase-shift analysis of finely stepped excitation functions and angular distributions of the $^{12}C+^{12}C$ elastic scattering yields spin information on both intermediate and gross structure resonances. To remove more ambiguities from the phase shift analysis, we are extending our analysis over a wider range of energies. This analysis of the $^{12}C+^{12}C$ elastic scattering combined with measurements of the $\alpha+^{20}Ne^*$ reduced widths will, hopefully, clarify the origin of resonant phenomena in the $^{12}C+^{12}C$ system.

ACKNOWLEDGMENTS

The authors would like to thank Professor J. J. Kolata for his total reaction cross section data prior to publication, and Professor H. Voit and Professor H. Emling for computer tapes of their elastic data. Discussions with Professor H. Feshbach, Professor A. Kerman, and Professor S. Y. Lee were very helpful and are gratefully acknowledged. This work was supported by the U.S. Department of Energy, under Contract No. ACO-2-76ER03069, and by FACESP, Brazil.

---

*Permanent address: Instituto de Fisica, Universidade de São Paulo, C.P. 20516, Brazil.

[1]K. A. Erb, R. R. Betts, S. K. Korotky, M. M. Hindi, P. P. Tung, M. W. Sachs, S. J. Willett, and D. A. Bromley, Phys. Rev. C 22, 507 (1980), and references therein.

[2]S. K. Korotky, K. A. Erb, S. J. Willett, and D. A. Bromley, Phys. Rev. C 20, 1014 (1979).

[3]E. Almqvist, D. A. Bromley, J. A. Kuehner, and B. Whalen, Phys. Rev. 130, 1140 (1963).

[4]D. A. Bromley, J. A. Keuhner, and E. Almqvist, Phys. Rev. Lett. 4, 365 (1960); Phys. Rev. 123, 878 (1961); E. Almqvist, D. A. Bromley, and J. A. Kuehner, Phys. Rev. Lett. 4, 515 (1960).

[5]B. Imanishi, Nucl. Phys. A125, 33 (1969).

[6]W. Scheid, W. Greiner, and R. Lemmer, Phys. Rev. 25, 176 (1970).

[7]T. Matsuse, Y. Kondō, and Y. Abe, Prog. Theor. Phys. 59, 1009 (1978); T. Matsuse, Y. Abe, and Y. Kondō, *ibid.* 59, 1904 (1978); Y. Kondō, Y. Abe, and T. Matsuse, Phys. Rev. C 19, 1356 (1979).

[8]O. Tanimura, Phys. Lett. 90B, 204 (1980).

[9]G. J. Michaud and E. W. Vogt, Phys. Rev. C 5, 350 (1972).

[10]W. Reilly, R. Wieland, A. Gobbi, M. W. Sachs, J. V. Maher, R. H. Siemssen, D. Mingoy, and D. A. Bromley, Nuovo Cimento 13A, 897 (1973); W. Rielly *et al.*, *ibid.* 13A, 913 (1973).

[11]H. Emling, R. Nowotny, D. Pelte, and G. Schreider, Nucl. Phys. A211, 600 (1973).

[12]E. R. Cosman, T. M. Cormier, K. Van Bibber, A. Sperduto, G. Young, J. Erskine, L. R. Greenwood, and O. Hansen, Phys. Rev. Lett. 35, 265 (1975).

[13]L. R. Greenwood, R. E. Segel, K. Raghunathan, M. A. Lee, H. T. Fortune, and J. R. Erskine, Phys. Rev. C 12, 156 (1975).

[14]T. M. Cormier, J. Appelgate, G. M. Berkowitz, P. Braun-Munzinger, P. M. Cormier, J. W. Harris, C. M. Jachcinski, L. L. Lee, Jr., J. Barrette, and H. E. Wegner, Phys. Rev. Lett. 38, 940 (1977); T. M. Cormier *et al., ibid.* 40, 924 (1978).

[15]N. R. Fletcher, J. D. Fox, G. J. Kekelis, G. R. Morgan, and G. A. Norton, Phys. Rev. C 13, 1173 (1976).

[16]E. R. Cosman, R. Ledoux, and A. J. Lazzarini, Phys. Rev. C 21, 2111 (1980), and references therein.

[17]J. J. Kolata, R. M. Freeman, F. Haas, B. Heusch, and A. Gallman, Phys. Rev. C 21, 579 (1980).

[18]P. Sperr, T. H. Braid, Y. Eisen, D. G. Kovar, F. W. Prosser, Jr., J. P. Schiffer, S. L. Tabor, and S. Vigdor,

Phys. Rev. Lett. 37, 321 (1976); D. G. Kovar *et al.* Phys. Rev. C 20, 1305 (1979).

[19]D. Shapira, R. G. Stokstad, and D. A. Bromley, Phys. Rev. C 10, 1063 (1974).

[20]H. Feshbach, J. Phys. (Paris) C 5, 177 (1976); MIT Internal Report CTP No. 671, 1977 (unpublished).

[21]G. Leander and S. E. Larsson, Nucl. Phys. A239, 93 (1975); I. Ragnarsson, S. Åberg, and R. K. Sheline, Contribution to Nobel Symposium 50, Nuclei at Very High Spin, LUND-MPH-80/19, 1980 (unpublished).

[22]H. Wojciechowski, D. E. Gustafson, L. R. Medsker, and R. H. Davis, Phys. Lett. 63B, 413 (1976).

[23]W. Treu, H. Fröhlich, W. Galster, P. Dück, and H. Voit, Phys. Rev. C 22, 2462 (1980).

[24]H. Emling, R. Nowotny, D. Pelts, G. Schreider, and W. Weidenmeier, Nucl. Phys. A239, 172 (1975).

[25]K. A. Eberhard and K. G. Bernhardt, Phys. Rev. C 13, 440 (1976).

[26]S. Y. Lee, H. W. Wilschut, and R. Ledoux, Phys. Rev. C 25, 2844 (1982).

[27]L. J. Satkowiak, P. A. De Young, J. J. Kolata, and M. A. Xapsos, Phys. Rev. C 26, 2027 (1982).

[28]Y. Abe, T. Matsuse, and Y. Kondō, Phys. Rev. C 19, 1365 (1979).

[29]R. J. Ledoux, Ph.D. thesis, MIT, 1981 (unpublished); E. R. Cosman, R. J. Ledoux, M. J. Bechara, C. E. Ordonez, and H. A. Al-Juwair, in *Resonances in Heavy Ion Reactions,* edited by K. A. Eberhard (Springer, Berlin, 1982), p. 112; R. J. Ledoux *et al.* (unpublished).

[30]H. Chandra and U. Mosel, Nucl. Phys. A298, 151 (1978).